Morphology of Phosphonic Acid-Functionalized Block Copolymers Studied by Dissipative Particle Dynamics

Sudip Roy,*,† Dilyana Markova,‡ Avneesh Kumar,‡ Markus Klapper,‡ and Florian Müller-Plathe†

Eduard Zintl Institut für Anorganische and Physikalische Chemie, Technische Universität Darmstadt, Petersenstrasse 20, 64287 Darmstadt, Germany, and Max-Planck-Institute for Polymer Research, Ackermannweg 10, D-55128 Mainz, Germany

Received October 9, 2008; Revised Manuscript Received December 2, 2008

ABSTRACT: Dissipative particle dynamics simulations were performed on phosphonic acid-functionalized copolymer melt. This copolymer consists of poly(ether−ether−ketone) and poly(*p*-vinylbenzylphosphonic acid) blocks. Three different mapping schemes were implemented to obtain the morphology in different length scales. The morphology obtained from the simulation of the copolymer when mapped in correspondence to experimentally obtained polymer showed a similar morphology to that obtained from scanning tunneling and atomic force microscopy. The simulations show that the poly(ether−ether−ketone) blocks aggregate in small clusters embedded by poly(*p*-vinylbenzylphosphonic acid) blocks. Two further mapping schemes were undertaken to elucidate the phase behavior in *p*-vinylbenzylphosphonic acid blocks in molecular scale. The results obtained from the simulations as well as the new identified morphologies provide useful information for synthesizing a new set of polymers which could be important to show promise for fuel cell application.

1. Introduction

Poly(*p*-vinylbenzylphosphonic acid) (PVBPA, cf. Figure 1) and its copolymers are among the materials with potential as fuel cell membranes in dry conditions and at high temperatures. Fuel cell electrode membrane assemblies (EMA) are currently receiving significant scientific attention as a possible next-generation energy source.[1−3] Fuel cells are already being used as an energy source for space technology, automation, and heating systems.[4−7] Recently, fuel cells have also been regarded as promising for automotive applications. Their main component is the EMA, which converts hydrogen into electrical energy and water as a byproduct. In commonly used fuel cells, the EMA consists mainly of platinum electrodes and liquid phosphoric acid as the electrolyte. However, due to the drawbacks of phosphoric acid, proton-conducting polymers, such as polymer electrolyte membranes (PEM), are being introduced as alternatives. PEMs are better than most other materials because of their light weight and their stability against the fuel cell's electrochemistry. The perfluorosulfonate ionomers such as DuPont's Nafion is at present the most widely used polymeric membrane. It has, however, several disadvantages. Its main drawback is that it is only operational at low temperatures (below 100 °C) because the proton transfer in this material occurs through a water phase. Above 80 °C, water starts to evaporate and the conductivity decreases. Therefore, efforts to improve proton conductivity under dry conditions have evolved several strategies[8] that employ alternative ionomers, such as phosphonic acid and sulfonic acid groups, to functionalize the polymer backbone. Such polymers conduct protons in dry conditions by structural hydrogen-bond networks.

The parent phosphonic acid is an amphoteric inorganic acid. It can be covalently linked to an aliphatic or aromatic spacer group and copolymerized with another polymer backbone, such as polystyrene or poly(ether−ether−ketone) (PEEK), to achieve better mechanical stability. The methylphosphonic acid unit can be conveniently placed on a styrene group and polymerized.[9]

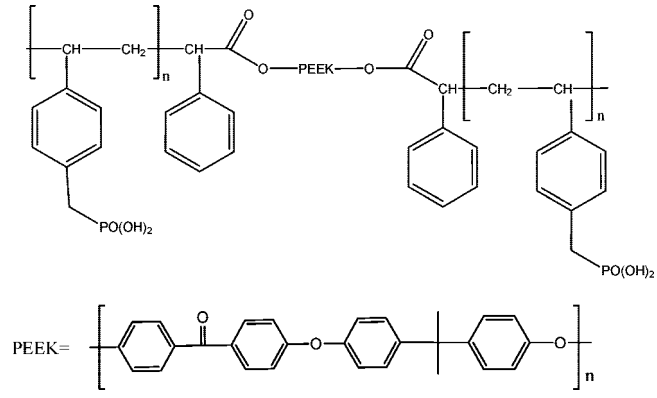

Figure 1. Block copolymer of poly(vinylbenzylphosphonic acid) and poly(ether−ether−ketone).

This proton-conducting polymer can be copolymerized with other polymers such as PEEK, which have no proton conductivity but provide the material with mechanical stability. The block copolymerization of the two polymers leads to different morphologies[10] with different proton conductivities. The morphology will depend on the volume fractions of the two components, on the block sizes, and on the topology and connectivity of the blocks.

The morphologies are a consequence of the segregation of different units, while the chemical link between them prevents macroscopic phase separation. The system tries to reduce its interfacial free energy by collecting similar beads in domains of different sizes and shapes such as sheets, rods, spheres, etc. The principles of this phenomenon have been described by Bates and Fredrickson.[11] However, the first theoretical study was done by Leibler[12] to understand the phenomena at different thermodynamic conditions using Gaussian coil statistics to calculate the free energy in the framework of Landau theory. Several different simulation models have subsequently been created to calibrate such systems and to understand the formation of complex morphologies. The first attempts used Monte Carlo simulations of lattice polymers,[13−15] but the system sizes were too small to understand the systems in their long-range behavior.

* Corresponding author. E-mail: s.roy@theo.chemie.tu-darmstadt.de.
† Technische Universität Darmstadt.
‡ Max-Planck-Institute for Polymer Research.

10.1021/ma802263t CCC: $40.75
Published on Web 01/06/2009

Alternatively, the polymer melt can be simulated off lattice by many simulation strategies, e.g., dynamic mean-field density functional methods,[16] coarse-grained molecular dynamics for relatively small size systems,[17] Brownian dynamics (BD),[18] and dissipative particle dynamics (DPD).[19] While DPD and BD both produce the correct equilibrium distributions of polymer chains in the melt, DPD has the additional advantage of correctly describing the hydrodynamic interactions.[19] In this research, we use DPD, which is similar to other molecular simulation techniques; i.e., the polymer chains are simulated in three dimensions using a parametrized force, and a Newton-like equation of motion updates the positions of the particles. In the context of this work, the main advantage of DPD is its use of beads (a collection of atoms according to their functional group), which remove the time-consuming hard-core repulsive interaction from the model. In DPD as formulated by Groot and Warren,[20] the particles interact via soft forces and, consequently, the polymer chains can pass through each other. This allows faster equilibration and a much longer time step than in straightforward molecular dynamics.[21] DPD has been successfully implemented for different real polymeric systems. The mesoscopic morphology of linear and graft-fluorinated block copolymers has been investigated by Özan et al.[22] Polyethylene and poly(L-lactide) polymer blends and diblock copolymers have been investigated as a function of chain length by Lee et al.[23] In addition to polymeric materials, DPD has also been used, for example, in the study of biomembrane morphology,[24] rupture of biomembranes by surfactants,[25] and the spontaneous vesicle formation in lipid bilayers.[26]

Block copolymers of the diethyl ester of PVBPA and poly(ether−ether−ketone) (PEEK) have been synthesized using PEEK macroinitiators.[27] The PEEK blocks are intended as a mechanical stabilizer and enable the copolymers to operate at higher temperatures without degradation of the material. The covalent link between the ionomer and the polymer backbone prevents the washing out of electrolyte material in fuel cell applications. According to the experimental studies of Klapper et al.[28] by atomic force microscopy (AFM) and scanning tunneling microscopy (SEM), phase separation is possible for high contents of PEEK. However, the AFM and SEM images also confirm that the presence of PEEK does not produce any formation of the (bi)continuous morphologies desired for good conductivity.

Synthesizing copolymer with discontinuous phases in the laboratory is difficult, and obtaining the desired three- dimensional morphology is demanding work. Since many target morphologies normally occur in a very narrow window of composition, molecular weight, and topology, mesoscale simulations are important and helpful for polymer chemists in designing their experiments. Therefore, DPD simulations are useful for predicting the morphologies beforehand for different copolymer architectures.

In this work, DPD simulations of the PVBPA−PEEK−PVBPA system are performed to investigate its phase morphology. This is a first step toward predicting phase morphologies for different block sizes, topologies, and connectivities and ultimately suggesting candidate copolymers for synthesis. A side aspect concerns the DPD model itself: different ways of coarse-graining the polymer under consideration are studied. DPD simulation of such a complex polymer necessarily involves parametrization of the cross-interaction parameters. This is done with the help of molecular dynamics simulations.

2. Theoretical Background

The DPD scheme was initially introduced by Hoogerbrugge and Koelman.[29] In DPD, a number of atoms are coarse-grained into a single DPD bead according to their chemical identity and their environment. The beads interact with each other by pairwise additive forces that locally conserve momentum and lead to the correct hydrodynamics.[30] A particle i at position r_i surrounded by particles $j \neq i$ at r_j (distance vector $r_{ij} = r_i - r_j$ and unit vector $\hat{r}_{ij} = r_{ij}/|r_{ij}|$) experiences a force with the components

$$f_i = \sum_{j \neq i} (F_{ij}^{C} + F_{ij}^{R} + F_{ij}^{D}) \tag{1}$$

where the sum runs over all the particles within a cutoff radius r_c. The conservative force is a soft repulsive term that acts along the line of the centers and is given by

$$F_{ij}^{C} = \begin{cases} a_{ij}\left(1 - \dfrac{r_{ij}}{r_c}\right)\hat{r}_{ij} & (r_{ij} < r_c) \\ 0 & (r_{ij} \geq r_c) \end{cases} \tag{2}$$

In eq 2, a_{ij} is the maximum repulsion between particles i and j. The second component of the force is a random force

$$F_{ij}^{R} = \sigma\left(1 - \frac{r_{ij}}{r_c}\right)\zeta_{ij}\hat{r}_{ij}/\sqrt{\mathrm{d}t} \tag{3}$$

the third one is a dissipative force

$$F_{ij}^{D} = -\gamma\left(1 - \frac{r_{ij}}{r_c}\right)^2(\hat{r}_{ij}\cdot v_{ij})\hat{r}_{ij} \tag{4}$$

In eq 3, ζ_{ij} is a randomly fluctuating variable that has a Gaussian statistic with a zero mean and a variance of one. In eq 4, the relative velocity of the two particles $v_{ij} = v_i - v_j$ and the friction coefficient γ are related to the magnitude of the random force σ by $\sigma^2 = 2\gamma k_B T$. This set of interacting particles is evolved in time using Newton's equation of motion. For simplicity, the mass of each particle is set to 1 and the cutoff radius r_c is considered to be 1, which is the basic unit of length of the system. With $k_B T = 1$ defining the unit of energy, the time unit becomes $\tau = r_c(m/k_B T)^{1/2}$. The velocity-dependent dissipative force F_{ij}^{D} provides a viscous drag to the particles, whereas the random term F_{ij}^{R} counteracts this cooling by applying random kicks to the particles that tend to increase the relative velocities of the adjacent pairs. Therefore, the combination of drag and random force provides a thermostat for the system.

The DPD beads represent several real atoms or monomers. Therefore, atomic level detail is neglected while interactions between different types of beads are the main parameters for defining a system. In eq 2, a_{ij} is the interaction parameter with the dimension of a force. As the conservative force (F_{ij}^{C}) is purely repulsive, liquid−vapor interfaces cannot be simulated, but in constant-volume ensembles liquid−liquid or solid−liquid interfaces can be simulated. In this sense, it is similar to the Flory−Huggins theory of lattice polymers. This theory is mainly used to estimate the free energy of mixing different types of particles or beads. The theory is extended to polymers by assuming that the beads are connected in a chain. The free energy of mixing such a system with two types of beads A and B can be written

$$\frac{\Delta G_{mix}}{RT} = \left(\frac{\phi_A}{N_A}\right)\ln \phi_A + \left(\frac{\phi_B}{N_B}\right)\ln \phi_B + \chi_{AB}\phi_A\phi_B \tag{5}$$

In eq 5, ϕ_A and ϕ_B represent the volume fraction for beads of type A and B, respectively. The first two terms in eq 5 describe the entropy of mixing which depends on the different ways that the chains can pack randomly on a lattice. The third term contains the mixing enthalpy, with χ_{AB} being the Flory−Huggins

parameter. Once the Flory−Huggins parameter is known for a system, the entire phase diagram can be calculated within the Flory−Huggins approximation.

The interaction parameter a_{AB} of the DPD conservative force can be mapped onto the Flory−Huggins χ_{AB} parameter by a simple linear equation suggested by Groot and Warren.[20] To derive the relationship, they run simulations of mixing two different types of beads (A and B) with different interaction parameters (a_{AB}). After equilibration the volume fraction of A in the majority of B phase is measured. These volume fractions (ϕ) are inserted into the following mean-field expression (eq 6) to get the χ_{AB}.

$$\chi_{AB} = \frac{\ln(1 - \phi) - \ln \phi}{1 - 2\phi} \tag{6}$$

Equation 6 is valid if the interaction parameters for similar beads are considered to be equal, i.e., $a_{AA} = a_{BB}$(interaction parameters for similar beads). Groot and Warren[20] reported the linear relation between excess interaction parameters Δa, i.e., $\Delta a = a_{AB} - a_{AA}$ and χ for different number densities.

$$\begin{aligned} \chi_{AB} &= (0.286 \pm 0.002)\Delta a \quad (\text{for } \rho = 3) \\ \chi_{AB} &= (0.689 \pm 0.002)\Delta a \quad (\text{for } \rho = 5) \end{aligned} \tag{7}$$

Groot and Warren[20] also calculated a similar linear relationship between Δa and χ for polymeric systems of chain length between 2 and 10

$$\chi_{AB} = (0.306 \pm 0.003)\Delta a \quad (\text{for } \rho = 3) \tag{8}$$

In the above two equations, the excess interaction parameter, which has a unit of energy per length, has been mapped to the dimensionless Flory−Huggins parameter. Therefore, the numerical preimplicitly carries the unit of length per energy in the above DPD reduced units.

The Flory−Huggins parameter can be estimated from Hildebrand solubility parameters δ in the following form[31]

$$\chi_{AB} \approx \frac{V}{k_B T}(\delta_A - \delta_B)^2 \tag{9}$$

where V is the average molar volume of the beads (or molecules) A and B. The solubility parameters are material-specific numbers and can be obtained from experiment or simulations. If experimental data are not available, one can, for example, perform atomistic molecular dynamic (MD) simulations to calculate the cohesive energy density (CED) from the nonbonded energy (molar enthalpy of vaporization) and the molar volume. The solubility parameters can then be obtained by the following equation suggested by Hildebrand

$$\delta_A = \left(\frac{\Delta H_{v,A}}{V_{m,A}}\right)^{1/2} = (\mathrm{CED}_A)^{1/2} \tag{10}$$

where $\Delta H_{v,A}$ is the molar enthalpy of vaporization and $V_{m,A}$ is the molar volume of bead A.

3. Computational Procedure

Model Building. The copolymer synthesized and characterized by the group of Klapper et al.[28] consists of two poly(vinylbenzylphosphonic acid) (PVBPA) blocks separated by a poly(ether−ether−ketone) (PEEK) block (Figure 1). The weight fraction of PEEK in the copolymer is about 1/7. For our DPD simulations we coarse-grained the whole polymer in three different ways.

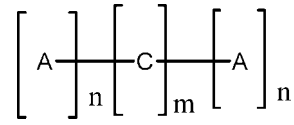

Figure 2. Model 1 treats the copolymer as a triblock of poly(vinylbenzylphosphonic acid) and poly(ether−ether−ketone) moieties.

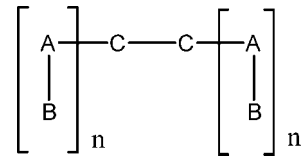

Figure 3. Model 2 treats the methylphosphonic acid groups (B) different from their styrene backbone groups (A). The comblike AB chains are attached to a central poly(ether−ether−ketone) block (C). The PEEK is treated as compatible to polystyrene (C = A).

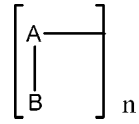

Figure 4. Model 3 neglects the (comparatively small) central block of poly(ether−ether−ketone) and treats the polymer as a comb of methylphosphonic acid groups (B) an a polystyrene backbone (A).

Model 1: Triblock Copolymer with Two Types of Beads. We considered PVBPA as block (segment) as a linear combination of bead A and ether−ether−ketone as another bead C. These two types of beads produce a $A_nC_mA_n$ triblock copolymer (Figure 2). In this way, we obtained a model in which beads represent segments. Experimentally obtained polymers have a typical molecular weight of 85 000 g/mol, where the molecular weight of the blocks with A and C beads are 36 500 and 12 000 g/mol, respectively. In our calculation we considered $n = 6$ and $m = 2$; i.e., each A bead corresponds roughly to a molecular weight of 6080 g/mol and each C bead to 6000 g/mol. The number of beads in each segment ($n = 6$ and $m = 2$) was chosen as an input value to build the model polymer chain of a certain size. This model emphasizes the copolymer as a classical A−C−A triblock.

Model 2: Grafted Copolymer with Three Types of Beads. In this mapping we additionally split the vinylbenzylphosphonic acid into a "methylphosphonic acid bead" and a "polystyrene bead", arriving at three bead types (Figure 3). Two like beads (C) were used to map ether−ether−ketone, and two other bead types were used to map styrene (A) and methylphosphonic acid (B). In this model we used the same interaction parameter between A and C bead, i.e., A = C. But due to the presence of C beads, the topology of the chain is different and represents a triblock copolymer where the outer blocks contain repeat units of two incompatible beads grafted on each other, symbolically $(AB)_n-C_2-(AB)_n$. For this model, we simulated $n = 3$ and $n = 6$ systems. The model emphasizes the difference between the polar phosphonic acid (B) and the nonpolar backbone (A, C). It does not differentiate further the two nonpolar components.

Model 3: Grafted Copolymer with Two Types of Beads. This model is the same as model 2 but without the C beads. It neglects the PEEK blocks altogether because of their low concentration. It constructs the polymer as if methylphosphonic acid beads were grafted on each monomer of polystyrene backbone. Bead A represents styrene and bead B represents methylenephosphonic acid (Figure 4), symbolically $(AB)_n$, with $n = 5, 10, 15$.

Table 1. Hildebrand Solubility Parameters for Bead A (Styrene/Ethylbenzene) and B (Methylphosphonic Acid) for Models 2 and 3

bead (models 2 and 3)	solubility parameter $(J/cm^3)^{1/2}$	molar volume (cm^3/mol)
A	20.0	114.6
B	26.3	62.5

Table 2. DPD Interaction Parameters in k_BT/r_c for Model 1

a_{ij}	A	C
A	25	28, 35, 45, 55
C	28, 35, 45, 55	25

Simulation Details. *Atomistic Molecular Dynamics Simulations.* We performed atomistic molecular dynamics (MD) simulations to calculate the solubility parameter from cohesive energy densities for styrene and methylphosphonic acid beads, which is the most crucial interaction in our copolymer. This was done because experimental solubility parameters are not available. Ethylbenzene and methylphosphonic acid act as model compounds to parametrize the interaction of beads A and B in models 2 and 3. Separate *NPT* MD simulations of 500 molecules of each type were carried out at ambient temperature (300 K) and pressure (1 bar). Periodic boundary conditions with a cutoff radius of 9 Å for ethylbenzene and 10 Å for methylphosphonic acid were used for nonbonded interactions. The force field of ethylbenzene was adapted from the polystyrene force field of ref 32. For methylphosphonic acid, the force field is taken from our simulations of heptylphosphonic acid.[33] The heat of vaporization was calculated separately for each type of molecule. The molar volume of each compound was calculated by dividing the molecular weight of the bead by the density obtained from *NPT* molecular dynamics. The experimental density for methylphosphonic acid was unknown. Therefore, molar volumes for both beads were calculated by MD simulations. In Table 1, the solubility parameters δ_A and δ_B calculated by eq 10 are reported. The calculated value of χ parameter (1.41) from the solubility parameters, which is greater than zero, indicates that ethylbenzene and methylphosphonic acid should not mix. To verify this, we also undertook a routine classical MD simulation of a mixed system of methylphosphonic acid and ethylbenzene. 250 molecules of both compounds were simulated with the above-mentioned force fields at a temperature of 300 K and a pressure of 1 bar from a randomly generated mixed system. From the simulation we observed complete phase separation of these two components.

DPD Simulations. The DPD interaction parameters are reported in Table 2. The DPD interaction parameters for models 2 and 3 were determined from atomistic simulations as described above. For model 1, the determination of interaction parameter from MD simulations would be too time-consuming because of the much larger bead size. On the basis of information from experimental studies that PVBPA and PEEK segregate, we therefore used a cross-interaction parameter which is much larger than the interaction parameter between like beads. DPD simulations of different model polymers were done for all the model systems as described above. All simulations were carried out in periodic boundary condition. Cubic boxes of different sizes were used. The number density for all the simulations was fixed at 3. We selected this density to be able to use eq 8 (which is derived only for number density 3 by Groot and Warren[20]) for converting the Flory−Huggins solubility parameter into the DPD interaction parameter. The bead masses and simulation temperatures (k_BT) are always set to unity as in the DPD model described by Groot and Warren.[20] The noise amplitude σ for the thermostat was set to 3 for all the simulations. For updating the positions we used the Lowe−Andersen integrating scheme,[34] which has been successfully tested for DPD simulations.[35] The Lowe−Anderson integrator is also a thermostat and hence can affect the Brownian-type dynamic of DPD particles. This issue already been examined by Noguchi and Gompper[36] where they have reported different dynamical properties as a function of DPD time step and with Lowe−Anderson thermostat. But in our case dynamics is beyond our main goal of investigation. Depending on the chain length and model, the total number of beads varies from 21 000 to 39 000 beads. In model 1, one chain consisted of 14 monomers, and we simulated 1500 chains. For model 2, the chains contained 14 and 26 monomers, and 1500 chains were simulated. In model 3 we undertook different simulations with different chain sizes, i.e., 10, 20, and 30 (in model $n = 5$, 10, and 15) monomers. The corresponding number of chains in the simulations was 2000, 1000, and 1000, respectively. Systems were always equilibrated initially for 10^6 DPD steps with a time step of 0.02τ. After these initial 10^6 DPD steps, the morphologies of the systems were recorded. The systems were then further simulated for another 10^6 steps. If the two morphologies were the same, then the last 10^6 steps were used for analysis. Most of the smaller systems (number of beads = 21 000) produced the same morphology after two cycles of 10^6 DPD steps. Systems with larger number of particles (30 000 and 39 000 beads) required a third cycle of 10^6 DPD steps. The morphologies of the systems were recorded from the last frame of the last cycle of the simulation.

Table 3. DPD Interaction Parameters in k_BT/r_c for Model 2

a_i	A	B	C
A	25	30, 35, 45, 55	25
B	30, 35, 45, 55	25	50
C	25	50	25

Table 4. DPD Interaction Parameters in k_BT/r_c for Model 3

a_{ij}	A	B
A	25	30, 35, 45, 55
B	30, 35, 45, 55	25

4. Results and Discussion

In models 2 and 3, bead A and bead B represent ethylbenzene (or styrene) and methylphosphonic acid fragments, respectively. The solubility parameters for these two types of beads were calculated by eq 10 from atomistic MD simulations (Table 1). From the solubility parameters, the Flory−Huggins χ_{AB} parameter was calculated to be 1.41 (eq 8). The χ_{AB} parameter is transformed to the DPD interaction parameter a_{AB} according to the following equation[20] for a number density of 3.0:

$$a_{AB} = a_{AA} + 3.27\chi_{AB} \tag{11}$$

In Tables 2, 3, and 4, we present all interaction parameters that were used for the conservative force in our DPD simulations for all the models. For models 2 and 3, $a_{AB} = 29.6$ is calculated from the atomistic MD simulations. We also carried out further DPD simulations with parameters larger than the calculated value to elucidate the effects of parameter variation.

The morphologies we obtained with these parameters are the same as the initial one which validates that we are already the segregation limit. In model 2 the interaction parameter between A and C bead is 25, which is the same as the interaction parameter between similar beads. Both beads A and C represent apolar thermoplastics, and they are compatible,[37] justifying the selection of the parameter. In the same model, the interaction parameter between B and C is the same as between B and A since a phosphonic acid fragment is interacting with two similar compatible polymers. From test simulations of model 1 with different parameters for A and C (not shown in detail), we found that the precise choice of a_{AB} has no effect on the morphology.

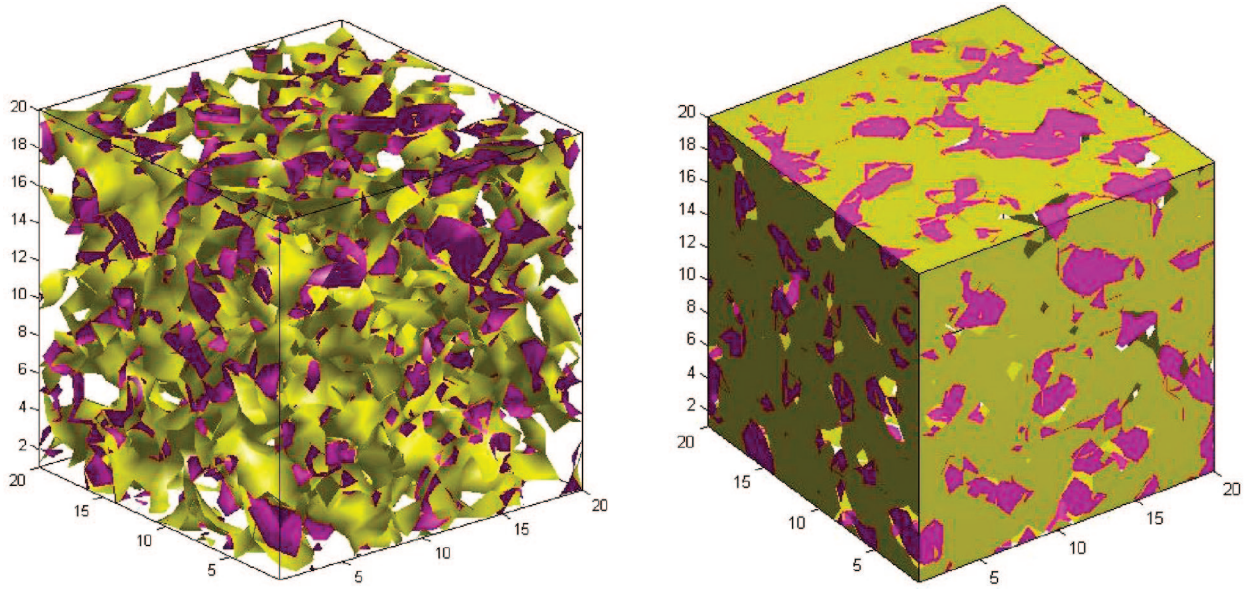

Figure 5. Morphology of model 1. A beads (poly(vinylbenzenephosphonic acid)) are in yellow and C (poly(ether−ether−ketone)) in purple. $\Delta a = 10k_BT$ has been used for the simulations shown in this figure.

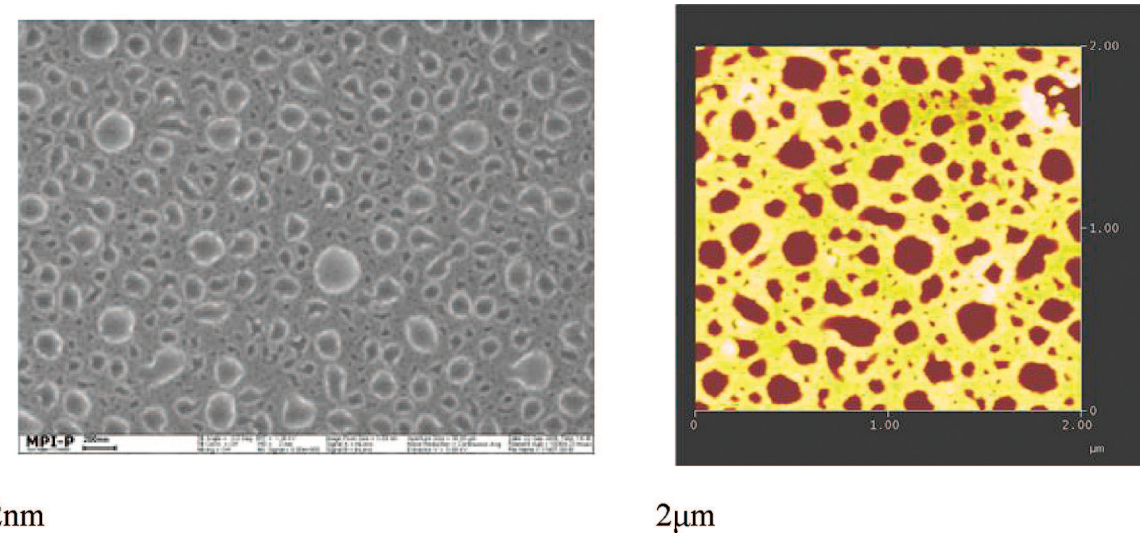

Figure 6. Experimental SEM (left panel) and AFM (right panel) images of the copolymer obtained by Klapper et al.[28] In the AFM picture, yellow represents poly(vinylbenzenephosphonic acid).

Parameter values in this range leave the system in the segregation limit, and small adjustments do not change this.

Morphology of Model 1. The model consists of two types of beads that are connected in blocks as $A_6-C_2-A_6$. The morphology obtained from this model is depicted in Figure 5. The left panel of the figure shows the morphology inside the simulation box, i.e., bulk material. The right panel shows the surface morphology which can be compared with experimentally obtained AFM and STM images. The interaction parameters used in the DPD simulations are reported in Table 2. The morphologies obtained using different settings of the parameter a_{AB} are similar. PEEK beads aggregate in small clusters, which are embedded in a PVBPA matrix; the PVBPA phase percolates (good for proton conductivity), and the PEEK phase does not (bad for mechanical stability). The experimental morphology is shown in Figure 6. Note that the SEM and AFM pictures were taken at different length scales. The morphology we obtained for this system is seen to be in agreement with the experimentally obtained morphology. The length scale of model 1 can be mapped onto the experimental systems using the relative molecular weights of the blocks.

Morphology of Model 2. In model 1, two chemically different units (styrene and phosphonic acid) are lumped into one A bead. Model 2 now distinguishes between the polar methylphosphonic acid and the apolar styrene. The morphology of model 2 is reported in Figure 7. The morphology for a system with two PVBPA chains of length $n = 3$ is shown in Figure 7a,b and for $n = 6$ in Figure 7c,d. For model 2, there is also a phase separation between beads A (phosphonic acid) and B (styrene). Styrene (B) and PEEK (C) do not phase separate, as they were treated as one type of bead. For the shorter chains ($n = 3$), there is some separation, but no ordered structure develops (Figure 7a,b). For longer chains ($n = 6$), however, the system forms a structure which consists of rodlike micelles of methylphosphonic acid. These micelles are parallel and arranged in bundles. Two such bundles with directions at 90° interpenetrate each other, so that the superstructure is percolating both for the phosphonic acid and for the PS/PEEK matrix. Proton conduction

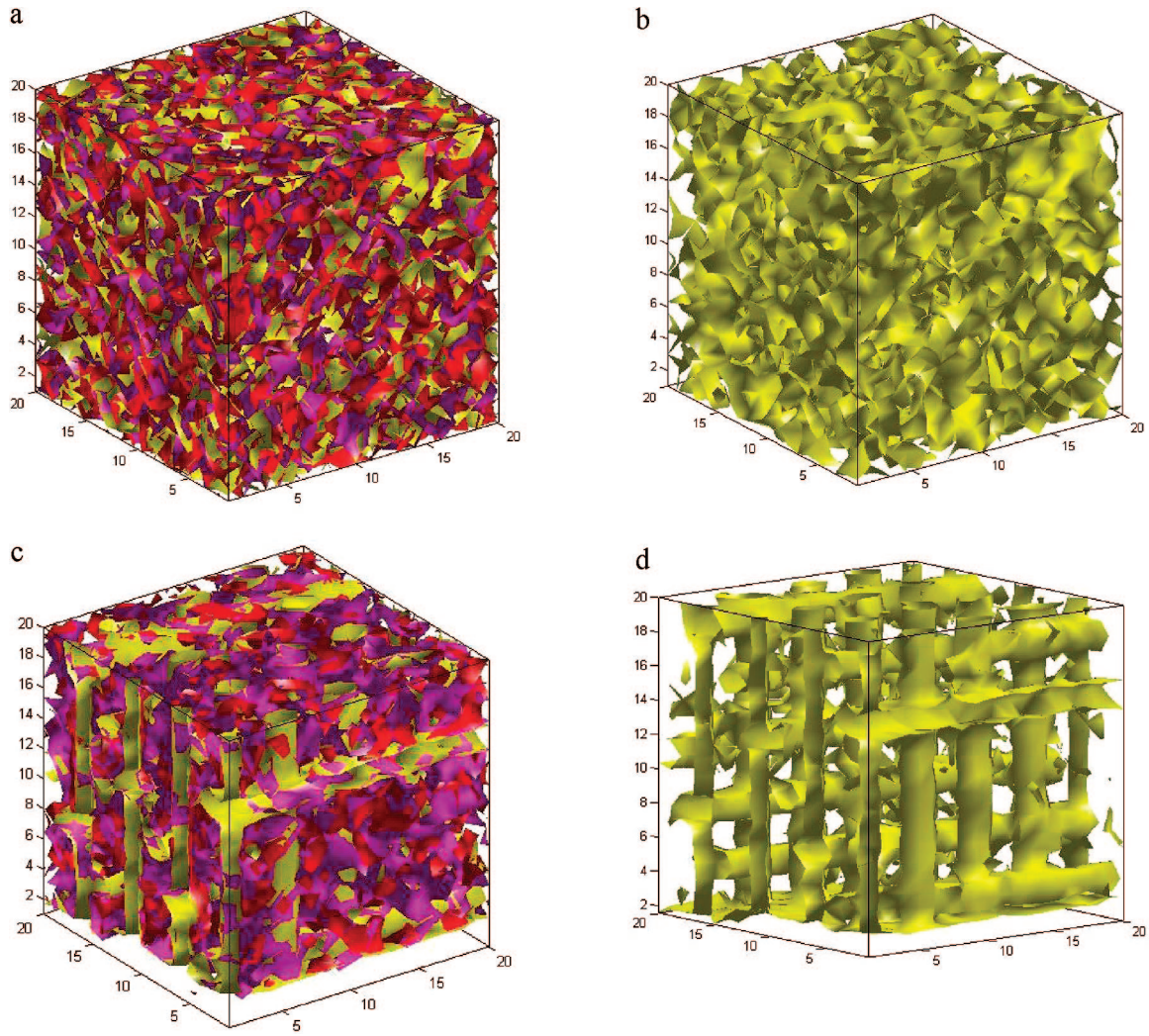

Figure 7. Morphologies of model 2: Panels a and b for chains with size $n = 3$; panels c and d for chains with size $n = 6$. In panels b and d, only bead B (methylphosphonic acid) is shown. Bead A (styrene) is red, B (methylphosphonic acid) yellow, and C (ether−ether−ketone) purple.

could proceed efficiently in the channels. This result indicates that there is probably a minimum length of the PVBPA blocks necessary to achieve ordered arrays of the channels.

Morphology of Model 3. Model 3 is a development of model 2. First, the central PEEK block is omitted; second, the remaining polymer (PVBPA) is investigated with different lengths. This means that the influence of PEEK can be investigated just by comparing model 2 and model 3. The number of binary units is $n = 5$, i.e., shorter than the shortest chain of model 2 (in model 2, $n = 3$ translates into 8 backbone beads because there are 2 outer blocks of length 3 and the inner block of length 2). The second size is $n = 10$, i.e., slightly longer than the chain of model 2; the longest chain has $n = 15$, i.e., about twice as long as the chain of model 2. We observe in Figure 8 that all chain lengths show phase separation. The chain length influences the morphology. The shorter chains produce no ordered superstructure (however, even $n = 5$ shows bicontinuity, Figure 8a,b). The longest chain reproduces the rodlike micelles from model 2. In model 3, however, they are less ordered and pronounced. (In Figure 8e,f, they are further obscured because one array happens to be orientated along one of the cube diagonals.) Comparing models 2 (central block of monomers compatible with backbone) and model 3 (no such central block, comb structure everywhere) indicates that the central PEEK block already helps to create a more orderly superstructure for shorter chain lengths.

Influence of the Model Parameters. The phase morphologies of all models are robust with respect to a change in the repulsion parameter of unlike beads. We performed variations of the cross-interaction parameters (Table 2) and found the morphologies unchanged. This indicates that for all settings of these parameters the strong-segregation regime is attained. This finding is borne out by the radii of gyration (Figure 9), which for each model is virtually independent of the respective interaction parameter for both models 1 and 2. The radius of gyration shows, however, the expected dependence on the length of the polymer for model 3 (Figure 10).

5. Conclusions

The phase morphology obtained for a simplified DPD model of the PVBPA/PEEK copolymer depends on the way the coarse-grained model is set up. Treating the copolymer as a classical incompatible A−C−A triblock (model 1) yields spherical micelles of PEEK domains in a matrix of PVBPA. This corresponds to the experimental structure. We therefore conclude that the repulsion of PVBPA and PEEK dominates the structural behavior of this copolymer. When PVBPA is treated as a polymer of a polystyrene backbone and incompatible covalently attached phosphonic acid moieties, rodlike micelles of phosphonic acid in a polystyrene matrix are obtained for long enough chains. The micelles are arranged into crossed parallel arrays whether there is a central PEEK block (model 2) or not (model

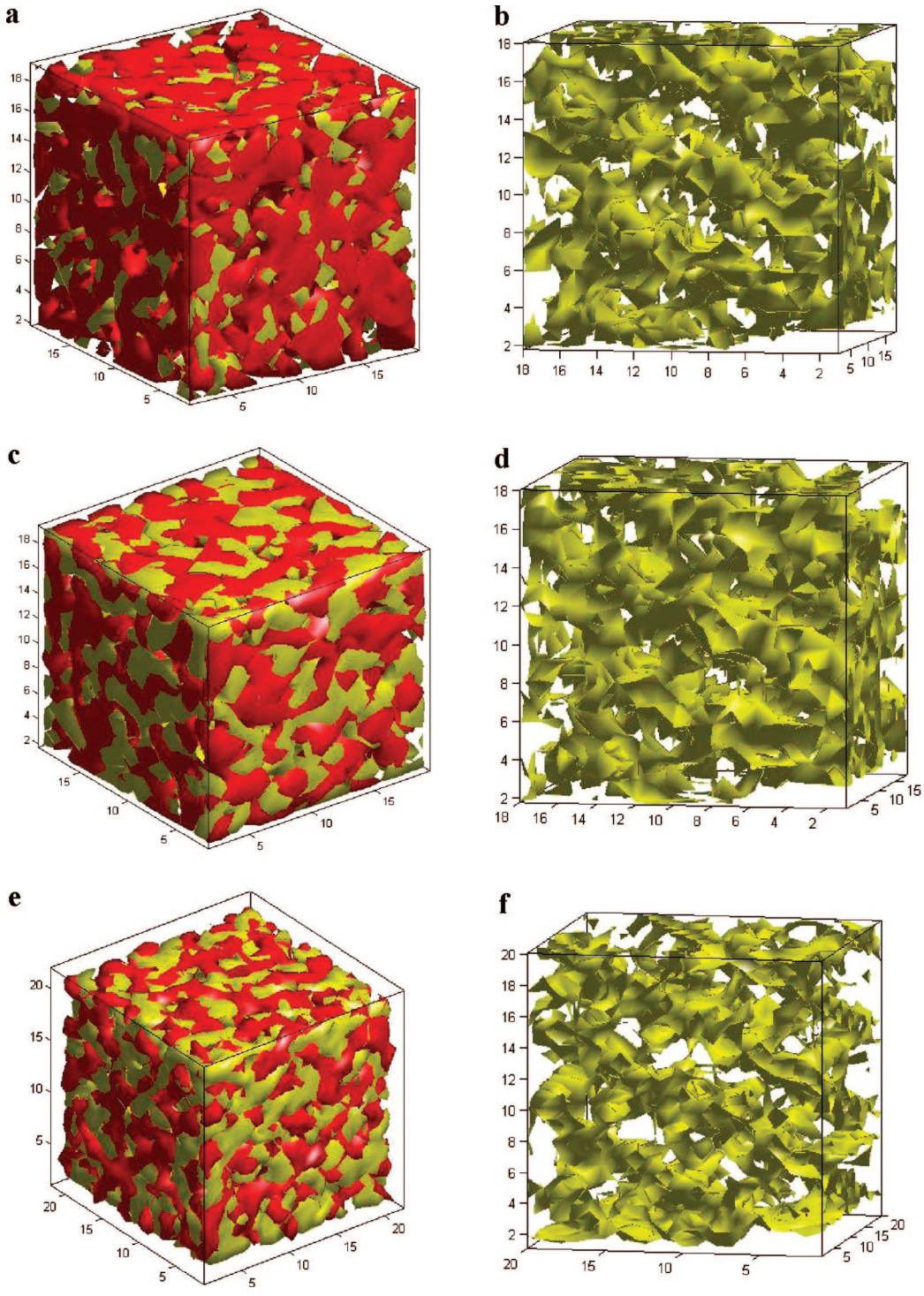

Figure 8. Morphologies of the grafted copolymer (model 3): panels a and b for chain length $n = 5$; panels c and d for chain length $n = 10$; panels e and f for chain length $n = 15$. Bead A (styrene) is red and B (methylphosphonic acid) yellow.

3). The central PEEK block, however, seems to promote ordering, but neither the morphology of model 2 nor that of model 3 is found in experiment. This suggests that in reality the phase separation between styrene and phosphonic acid cannot occur, in spite of the known (from the atomistic calculations) incompatibility between the two moieties. The reason can therefore only be the small size of the two moieties. Even if several neighboring phosphonic acids come together, they may cluster, but this cluster is not large enough to show up as a thermodynamic phase in an AFM picture. The DPD model, in contrast, tacitly assumes that each of its beads is a sizable portion of a polymer chain. This assumption is certainly not fulfilled for PVBPA.

On the other hand, the calculations also show the way forward to a bicontinuous morphology, where both phases percolate. A comb topology with phosphonic acid-bearing chains grafted onto an incompatible backbone should lead to the interpenetrating arrays of rods, provided the molecular weights of the arms are comparable to the molecular weight of backbone strands between two attachment points. The arms could again consist of PVBPA; the backbone must be incompatible with it.

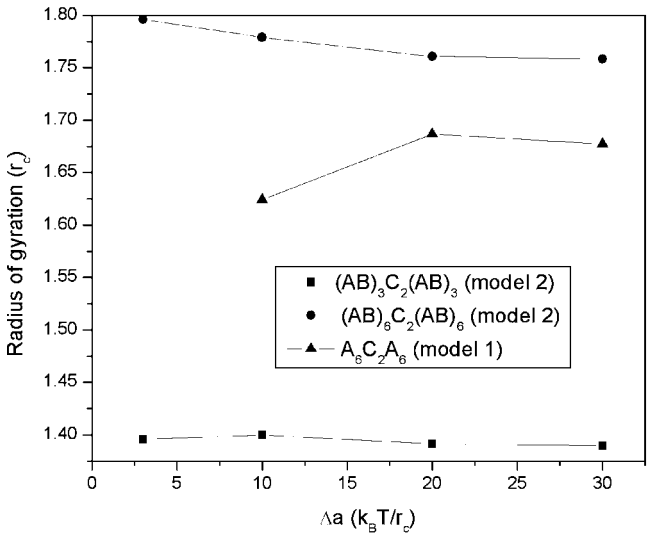

Figure 9. Radius of gyration as a function of excess interaction parameter between A and B beads for models 1 and 2.

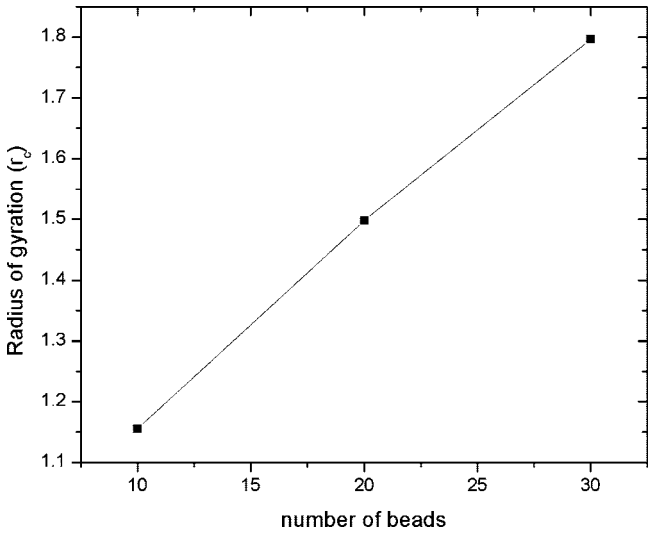

Figure 10. Radius of gyration as a function of the number of beads for model 3.

DPD simulations are able to attain the morphologies which are experimentally observed and can also be used to predict three-dimensional morphologies for different block lengths and polymer architectures. It is, therefore, a useful method and can be used as a prediction tool for synthesizing new polymer materials of certain target morphology.

Acknowledgment. We thank Tinashe Ndoro for a critical reading of the manuscript. This work has been supported by the DryD project of the German Bundesministerium für Bildung and Forschung (035F0309F).

References and Notes

(1) Steininger, H.; Schuster, M.; Kreuer, K. D.; Kaltbeitzel, A.; Bingol, B.; Meyer, W. H.; Schau, S.; Brunklaus, G.; Maier, J.; Spiess, H. W. *Phys. Chem. Chem. Phys.* **2007**, *9*, 1764.
(2) Gray, F. M. *R. Soc. Chem.* **1997**.
(3) Blomen, L. J. M. J. *Fuel Cell System*; Plenum: New York, 1993.
(4) Schuster, M.; Kreuer, K. D.; Steininger, H.; Maier, J. *Solid State Ionics* **2008**, *179*, 523.
(5) Hickner, M.; Ghassemi, H.; Kim, Y. S.; Einsla, B. R.; McGrath, J. E. *Chem. Rev.* **2004**, *104*, 4587.
(6) Rusanov, A. L.; Likhatchev, D.; Kostogolov, P. V.; Müllen, K.; Klapper, M. *Adv. Polym. Sci.* **2005**, *179*, 83.
(7) Kreuer, K. D.; Paddison, S. J.; Spohr, E.; Schuster, M. *Chem. Rev.* **2004**, *104*, 4637.
(8) Rikukawa, M.; Sanui, K. *Prog. Polym. Sci.* **2000**, *25*, 1463.
(9) Markova, D.; Kumar, A.; Müllen, K.; Klapper, M. *Prepr. Symp.—Am. Chem. Soc., Div. Fuel Chem.* **2006**, *52*, 651.
(10) Yang, Y.; Holdcroft, S. *Fuel Cells* **2005**, *5*, 171.
(11) Bates, F. S.; Fredrickson, G. H. *Annu. Rev. Phys. Chem.* **1990**, *41*, 525.
(12) Leibler, L. *Macromolecules* **1980**, *13*, 1602.
(13) Hoffmann, A.; Sommer, J. U.; Blumen, A. *J. Chem. Phys.* **1997**, *106*, 6709.
(14) Ko, M. B.; Mattice, W. L. *Macromolecules* **1995**, *28*, 6871.
(15) Larson, R. G. *Macromolecules* **1994**, *27*, 4198.
(16) Maurits, N. M.; Vlimmeren, B. A. C. v.; Fraaije, J. G. E. M. *Phys. Rev. E* **1997**, *56*, 816.
(17) Müller-Plathe, F. *ChemPhysChem* **2002**, *3*, 754.
(18) Groot, R. D.; Madden, T. J.; Tildesley, D. J. *J. Chem. Phys.* **1999**, *110*, 9739.
(19) Groot, R. D.; Madden, T. J. *J. Chem. Phys.* **1998**, *108*, 8713.
(20) Groot, R. D.; Warren, P. B. *J. Chem. Phys.* **1997**, *107*, 4423.
(21) Karttunen, M., Vattulainen, I., Lukkarinen, A., Eds.; *Novel Methods in Soft Matter Simulations*; Springer: Heidelberg, 2004; Vol. *640*.
(22) Özen, A. S.; Sen, U.; Atilgan, C. *J. Chem. Phys.* **2006**, *124*, 064905.
(23) Lee, W. J.; Ju, S. P.; Wang, Y. C.; Chang, J. G. *J. Chem. Phys.* **2007**, *127*, 064902.
(24) Shillcock, J. C. *J. Chem. Phys.* **2002**, *117*, 5048.
(25) Groot, R. D.; Rabone, K. L. *Biophys. J.* **2001**, *81*, 725.
(26) Yamamoto, S.; Maruyama, Y.; Hyodo, S. *J. Chem. Phys.* **2002**, *116*, 5842.
(27) Klapper, M.; LeGuen, A.; Hoffmann, U.; Wehrmeister, T.; Mullins, S.; Müllen, K. *Polym. Prepr.* **1997**, *38*, 66.
(28) Markova, D.; Kumar, A.; Klapper, M.; Müllen, K. *Polymer*, submitted.
(29) Hoogerbrugge, P. J.; Koelman, J. *Europhys. Lett.* **1992**, *19*, 155.
(30) Ripoll, M.; Ernst, M. H.; Español, P. *J. Chem. Phys.* **2001**, *115*, 7271.
(31) Hildebrand, J. H. *The Solubility of Non-Electrolytes*; Reinhold: New York, 1936.
(32) Müller-Plathe, F. *Macromolecules* **1996**, *29*, 4782.
(33) Roy, S.; Ataol, T. M.; Müller-Plathe, F. *J. Phys. Chem. B* **2008**, *112*, 7403.
(34) Lowe, C. P. *Europhys. Lett.* **1999**, *47*, 145.
(35) Chen, L.-J.; Lu, Z.-Y.; Qian, H.-J.; Li, Z.-S.; Sun, C.-C. *J. Chem. Phys.* **2005**, *122*, 104907.
(36) Noguchi, H.; Gompper, G. *Europhys. Lett.* **2007**, *79*, 36002.
(37) Wenz, L. M.; Mettitt, K.; Brown, S. A.; Moet, A.; Steffee, A. D. *J. Biomed. Mater. Res.* **1990**, *24*, 207.

MA802263T